JTTEE5 17:728–735
DOI: 10.1007/s11666-008-9254-5
1059-9630/$19.00 © ASM International

Peer Reviewed

Characterization of Low-Pressure Cold-Sprayed Aluminum Coatings

K. Ogawa, K. Ito, K. Ichimura, Y. Ichikawa, S. Ohno, and N. Onda

(Submitted May 14, 2008; in revised form September 22, 2008)

Aluminum alloys are widely used as materials for engineering components of automobiles and airplanes because of their light weight and high corrosion resistance. However, cracks may develop sometimes in aluminum components, which have to be repaired by welding. It is difficult to weld aluminum components due to its high specific thermal conductivity and high coefficient of thermal expansion. The low-pressure cold-spray technique can be used instead of welding for repairing cracks. However, the effects of surface conditions on particle deposition and the mechanical properties of cold-sprayed coatings have not been investigated thus far. In this study, the effect of surface conditions focusing on active newly formed surface on aluminum particle deposition is studied and the mechanical properties of low-pressure cold-sprayed aluminum coatings are investigated by four-point bending tests. It is found that for efficient particle deposition it was necessary to obtain active newly formed surface of the substrate and particle surfaces by several impingements because the existence of inactive native oxide films has an adverse effect on the deposition. Furthermore, the strength of a cold-sprayed specimen is found to be higher than that of a cold-rolled specimen under compressive loading.

Keywords low-pressure cold spray, aluminum, bonding strength, characterization, deposition mechanism, four-point bending tests, newly-formed surface

1. Introduction

Surfaces are widely coated to obtain the required surface conditions and properties. In the past, many coatings used have been applied using the thermal spray processes. In a conventional thermal spray process, the coating material is heated to the molten or semimolten state and impinged onto a substrate surface. Because of heating, thermal spray coatings show various unfavorable phenomena, e.g., oxidation, phase transformation, etc. A new coating technique, the cold-gas dynamic-spray process, often simply called "cold spray," was initially developed in the mid-1980s (Ref 1-5). This technique is based on the high-velocity impinging (300-1200 m/s) of minute solid particles (generally 10-50 μm in diameter) on a substrate (Ref 4-6). In this process, the powder particles are accelerated by a supersonic gas jet at a high gas temperature, which is usually lower than the melting point of the powder material. Consequently, cold spray has solved the problems encountered in the thermal spray process (Ref 7). Many researchers have carried out studies on cold-sprayed coatings formed at high pressures of the order of a few megapascals (Ref 8-10). Recently, low-pressure cold-spray equipment, operating at a pressure typically less than 1 MPa, has drawn some researchers' attention (Ref 11), because, the equipment for low-pressure cold-spraying is considerably simpler and smaller than the high-pressure cold-spray equipment. As a result, the application field for cold spray has become wider, e.g., low-pressure cold-spray equipment can be used for on-site maintenance. In particular, aluminum alloys are widely used as materials for engineering components of automobiles and airplanes because of their light weight and high corrosion resistance. However, cracks may develop in aluminum components sometime, which have to be repaired by welding and conventional thermal spray techniques. Cold spraying can be used an alternative technique to repair the cracks in aluminum components.

During cold spraying, solid particles are accelerated to high velocities and impinged onto a substrate. The impinged particles deform the substrate surface and form a new surface. This process plays an important role in the deposition. The kinetic energy of the high-velocity particles is an important factor on which the impingement, deformation, and deposition mechanisms depend. The critical particle velocity of a spray material under the

This article is an invited paper selected from presentations at the 2008 International Thermal Spray Conference and has been expanded from the original presentation. It is simultaneously published in *Thermal Spray Crossing Borders, Proceedings of the 2008 International Thermal Spray Conference*, Maastricht, The Netherlands, June 2-4, 2008, Basil R. Marple, Margaret M. Hyland, Yuk-Chiu Lau, Chang-Jiu Li, Rogerio S. Lima, and Ghislain Montavon, Ed., ASM International, Materials Park, OH, 2008.

K. Ogawa, K. Ito, K. Ichimura, and **Y. Ichikawa**, Fracture and Reliability Research Institute, Tohoku University, Aoba 6-6-01, Aramaki, Aoba-ku, Sendai 980-8579, Japan; and **S. Ohno** and **N. Onda**, Tohoku Electric Power Co., Inc., 1-7-1, Honcho, Aoba-ku, Sendai 980-8550, Japan. Contact e-mail: kogawa@rift.mech.tohoku.ac.jp.

high-pressure cold-spray conditions, which is the threshold particle velocity for adhesion/separation, has been numerically studied (Ref 12-16). Assadi et al. reported that the critical velocity of aluminum was 620-675 m/s in the case of high-pressure cold spray (Ref 12). In our previous study (Ref 17), it has been found that the critical velocity of the aluminum under low-pressure cold spray was approximately 300 m/s. The difference between the both critical velocities was almost twofold. Hence, the deposition mechanisms in low-pressure cold spraying may differ from those in high-pressure cold spraying each other.

In this study, the effect of surface conditions on low-pressure cold spraying was investigated. Further, to evaluate the mechanical properties of cold-sprayed coatings, the interfacial strength of the coatings was determined by four-point bending tests.

2. Experimental

2.1 Spraying System and Materials Used

In this study, the commercial cold-spray facility DYMET403J (Obninsk Center for Powder Spraying, Russia) was used for spraying. Since this equipment uses compressed air as the carrier gas, only an air compressor is required. Moreover, the main unit has a small built-in gas heating system that is used to heat the working gas directly; hence, the equipment is small and lightweight. A round-shaped exit nozzle with a diameter of 4.8 mm was used. Compressed air at 0.6 MPa was used as the carrier gas. Pure aluminum powder (Al G-AT, Fukuda Metal Foil & Powder Corporation) was used. The oxygen content of the particle was approximately 0.2%. The averaged particle diameter of the powder used in the study is 17.3 μm. A cold-rolled plate of pure aluminum alloy (A1050) with dimensions of 40 × 150 × 3 mm was used as the substrate. Due to formation of thick coating, 40 m/s was the traverse speed of gun for deposition efficiency measurements and making specimens of four-point bending tests. On the other hand, due to evaluation of deposition behavior of an independent particle, the traverse speed was 500 m/s in the cases of evaluation of number of particle deposited, and of effects of roughness and oxide films for deposition.

2.2 Evaluation of Number of Particles Deposited

To investigate the particle deposition phenomenon in the early stage, the specimens were impinged with limited particles. At a high traverse speed and low powder feed rate, it can be realized to make very limited particles impinge on a mirror-polished aluminum substrate. The surface roughness Ra of the substrate was 0.2 μm. The number of particles deposited on the substrate in a spray area (1 × 5 mm), as shown in Fig. 1, was determined by the scanning electron microscope (SEM) observation.

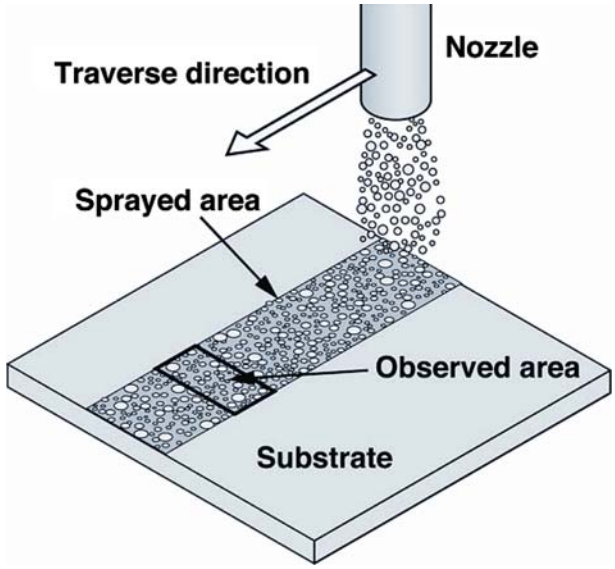

Fig. 1 Schematic illustration of measurement of number of particles deposited

2.3 Deposition Efficiency

The deposition efficiency (DE) of particles was measured as follows. Before spraying, the weights of the substrate (W_{s1}) and the feed stock powder (W_{p1}) were measured. Then, the weights of the sprayed substrate (W_{s2}) and the remaining feed stock powder (W_{p2}) were measured. Finally, the DE of particles was determined by using these measured values and Eq 1.

$$\mathrm{DE} = \frac{W_{s2} - W_{s1}}{W_{p2} - W_{p1}} \times 100\ (\%) \qquad \text{(Eq 1)}$$

It was difficult to measure the weight of the remaining feed stock powder because some powder remained inside the spraying equipment. This powder loss may introduce a measurement error. Therefore, we measured the average weight difference (M) between the input feed stock powder and take off powder. Using M, Eq 1 was modified to obtain Eq 2.

$$\mathrm{DE} = \frac{W_{s2} - W_{s1}}{W_{p2} - W_{p1} - M} \times 100\ (\%) \qquad \text{(Eq 2)}$$

Finally, the DE of particles was calculated using Eq 2.

2.4 Effect of Ra on Particle Deposition

To evaluate the effect of Ra on particle deposition, specimens with different Ra values, i.e., 0.2, 1.0, and 3.0 μm, were prepared. Then, the relationship between the number of particles deposited in the sprayed area (1 × 5 mm) and the number of traverses was investigated.

2.5 Effect of Native Oxide Film on Particle Deposition

Initial spraying can remove native oxide films. Therefore, to evaluate the effect of the formation of native oxide

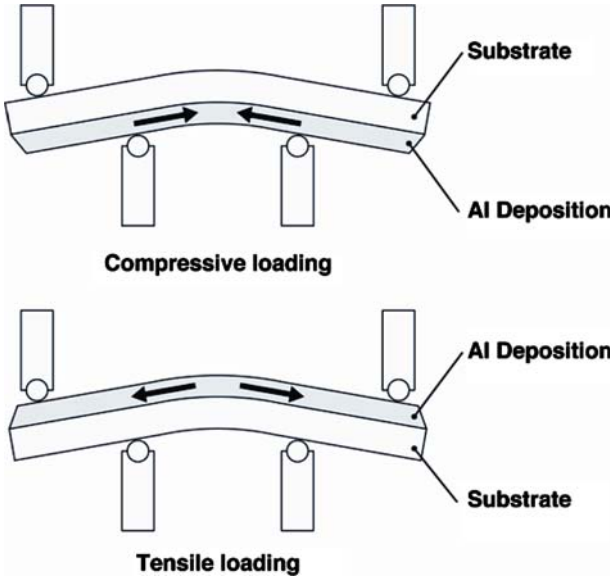

Fig. 2 Schematic illustrations of loading direction during four-point bending tests

films on particle deposition, specimens with different traverse intervals were prepared. The traverse intervals were set at 0.6, 60, 600, 1800, and 3600 s.

2.6 Four-Point Bending Tests

To evaluate the mechanical properties of the cold-sprayed coatings under tensile and compressive loadings, four-point bending tests were carried out.

Figure 2 shows the schematic illustration of the loading direction of the specimens under tensile and compressive loadings during the four-point bending tests. Under the four-point bending test, the maximum stress is always located on the surface. By cold spraying, 3 mm-thick pure aluminum coatings were formed on 3 mm-thick aluminum substrates. Then, a 1 mm-thick aluminum coating was removed by machining. Four-point bending specimens with dimensions of $5 \times 40 \times 5$ mm were prepared from the cold-sprayed specimens. Further, to compare bending force, cold-rolled aluminum specimens with a thickness of 5 mm were prepared. The specimens were subjected to four-point bending tests by using a servohydraulic testing machine with an inner span of 15 mm and an outer span of 34 mm at a crosshead speed of 0.6 mm/min. After the four-point bending tests, the fracture surfaces were observed by SEM.

3. Results and Discussion

3.1 Measurements of Number of Particles Deposited

Figure 3 shows the typical SEM images of the cold-sprayed specimens with different traverse numbers, and Fig. 4 shows the change in the number of particles deposited for different traverse numbers. In the case of the specimens with traverse numbers equal to 1 and 2, no particle deposition was observed on the substrates. For traverse numbers in the range of 6-12, the number of particles deposited increased slightly. This result indicates the presence of a time delay in particle deposition in low-pressure cold-spray deposition. The time delay causes changes in the substrate surface conditions, such as roughening and formation of a newly formed surface. The surface roughness influences elimination of the oxide film on the particle surface. And also, the formation of the newly formed surface, which was formed by several particle impingements, has higher surface energy, because of eliminating inactive oxide films. Therefore, it can be possible to improve bonding force. As a result of these changes, the DE of particles increases. The effects of surface roughness and newly formed surface are described in sections ''Effect of Ra on Particle Deposition'' and ''Effect of Formation of Newly Formed Surface on Particle Deposition'' in detail, respectively.

The time delay indicates that particle deposition by low-pressure cold spraying requires repeated impingements. Repeated impingements enhance particle deposition. Even though low-pressure cold spray exhibits low deposition efficiency, the velocity of particle deposition in low-pressure cold spray is lower than that in high-pressure cold spray. Further, the latter technique may not require repeated impingements because it has sufficient energy for making the newly formed surface due to the high-speed and high-pressure impingements. Accordingly, it is assumed that the difference in the critical velocities of low- and high-pressure cold sprays is due to the difference in the mechanism of active newly formed surface formation of the two techniques.

3.2 DE of Particles

Figure 5 shows the DE of low-pressure cold-sprayed aluminum coatings. The DE increases with the traverse number. At the early starting of the spraying, particle deposition was unstable. Therefore, the DE of less traverses may include influence of such unstable. However, after four traverses that have no effect of unstable, deposition gets saturated. Even for such case, the maximum spray efficiency of low-pressure cold spray is very low, approximately 7%, because it can be difficult to break oxide films and to form an active newly formed surface, due to low impingement force.

3.3 Effect of Ra on Particle Deposition

The relationship between the number of particles deposited and the traverse number for the specimens with different Ra values is shown in Fig. 6. From this figure, it is evident that the deposition in the specimens with Ra equal to 1.0 and 3.0 starts earlier than that of the specimen with Ra equal to 0.2. It is thought that Ra has a significant effect on deposition of coatings. However, the specimens with Ra equal to 1.0 and 3.0 show almost no difference in their coatings. From this result, it is assumed that particle depositions require a certain level of roughness.

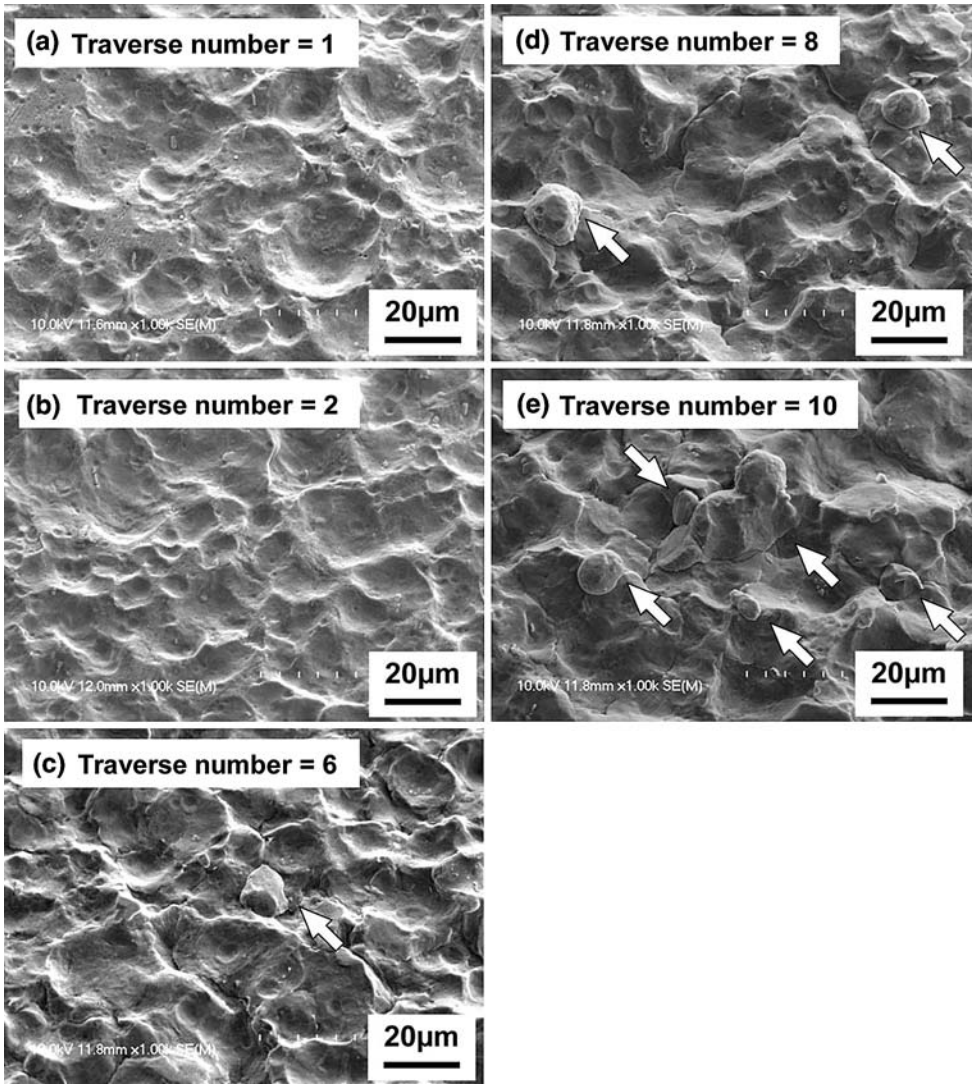

Fig. 3 Typical SEM images of substrate surfaces for different traverse numbers. (a) Traverse number = 1, (b) Traverse number = 2, (c) Traverse number = 6, (d) Traverse number = 8, and (e) Traverse number = 10. The white arrows indicate deposited particles

3.4 Effect of Formation of Newly Formed Surface on Particle Deposition

The relationship between the number of particles deposited and the traverse number for the specimens with different traverse intervals is shown in Fig. 7. Significant deposition is observed in the specimen with a short traverse interval. Thus, the removal of native oxide films, i.e., the formation of an active newly formed surface, is the key factor in the depositions. Further, the formation of native oxide films has an adverse effect on the deposition. Therefore, it is necessary to form a newly formed surface at the substrate surface for deposition. In the case of particle/particle deposition, it is also necessary to form a newly formed surface at the particle surface. With regard to the effect of newly formed surface, Tanaka et al. also reported that the formation of a newly formed surface directory improved joining of friction stir-welded aluminum/steel (Ref 18).

However, it was considered that the other factor such as the temperature rising during repeated scanning of the gun over the surface. Consequently, the temperature near the surface was measured by K-type thermocouple during the scanning of the gun, in the case of interval of 0.6 s. Schematic illustration of setup of the measurement is shown in Fig. 8. The result of the temperature measurement is shown in Fig. 9. As a result, only 2 °C temperature rising was observed. Therefore, it is thought that there is almost no temperature influence.

3.5 Four-Point Bending Tests

The results of the four-point bending tests are shown in Fig. 10. A comparison of the slopes of the plots of the cold-sprayed specimens and the cold-rolled aluminum specimens in the elastic region, shows that the former have higher elastic moduli as compared to the latter. In the case of compressive loading, the former showed a higher

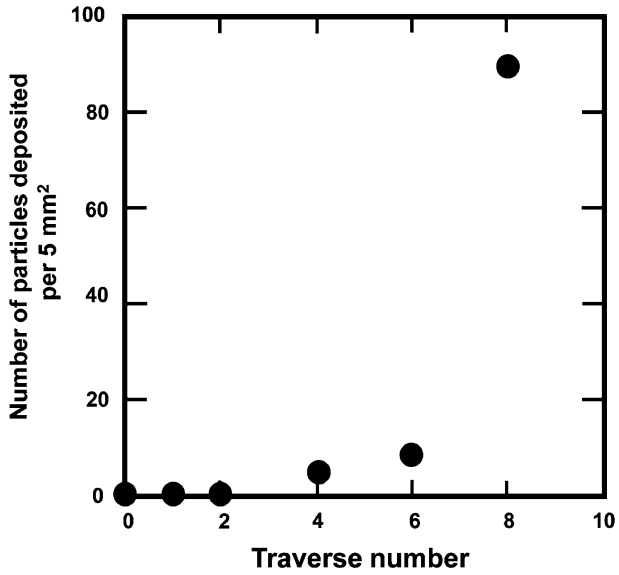

Fig. 4 Relationship between number of particles deposited and traverse number

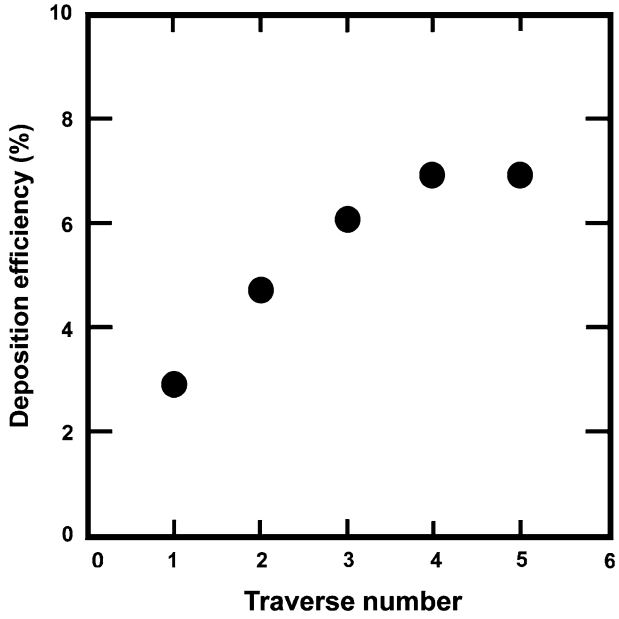

Fig. 5 Relationship between deposition efficiency and traverse number

strength as compared to the latter. In the case of tensile loading of the cold-sprayed specimens, the cold-sprayed coatings were found to be hardly ductile and fragment occurred after 0.2 mm displacement, leading to the unstable fractures.

The images of the specimens after the four-point bending tests are shown in Fig. 11. In the compressive loaded specimen, cracks were not observed in the deposited aluminum coating. On the other hand, in the tensile-loaded specimen, a vertical crack was suddenly initiated from the surface of the aluminum coating during loading,

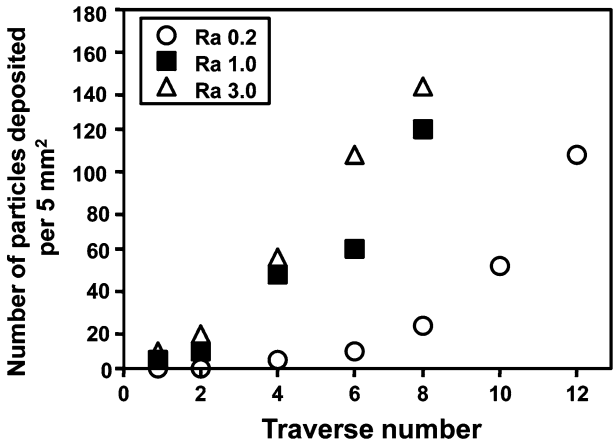

Fig. 6 Effect of surface roughness on particle deposition

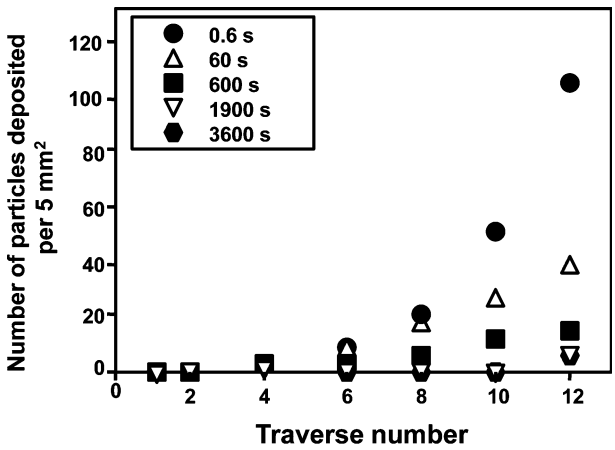

Fig. 7 Effect of traverse interval on deposition

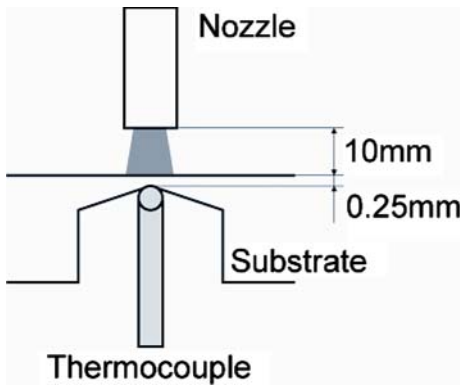

Fig. 8 Schematic illustration of temperature measurement

which propagated down to the interface between the aluminum coating and the substrate. Finally, a crack was formed along the horizontal direction. The point where the coating fractured (Fig. 10) possibly corresponded to the point at which the vertical crack initiated.

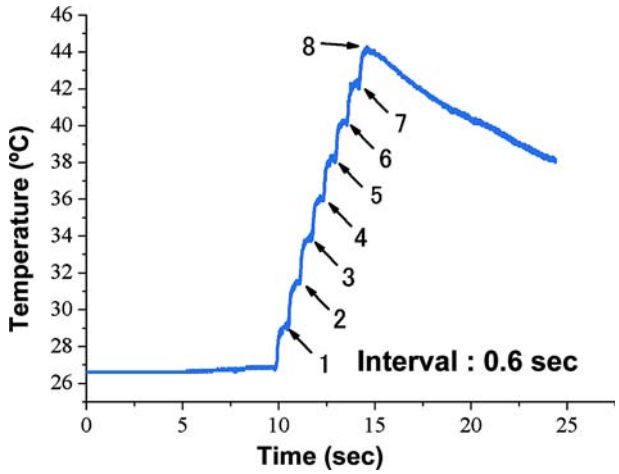

Fig. 9 Results of temperature measurement during scanning of the gun over the surface

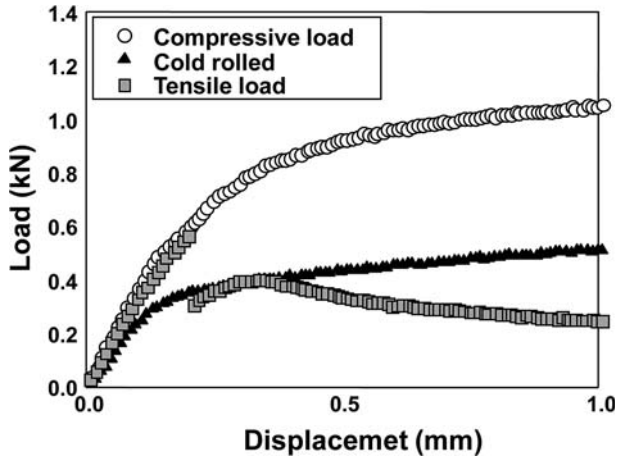

Fig. 10 Results of four-point bending tests

The sprayed particles are attracted toward the substrate or the deposited particles. A strong adhesion can be attained between the particles and the substrate and cohesion between the deposited particles. However, the cohesion between adjacent particles cannot be strong. Therefore, it is easy to initiate a vertical crack in the tensile loaded specimen. An SEM image of the fracture surface of the tensile loaded specimen after being subjected to the four-point bending test is shown in Fig. 12. In this figure, the deposited aluminum particles are indicated by arrows. Consequently, it is assumed that the cohesive strength between adjacent particles is weak. To improve the cohesive strength, the aluminum coatings were subjected to heat treatment.

To improve the strength of the specimens under tensile loading, they were subjected to heat treatment. The temperature for heat treatment of pure aluminum was set at 270 °C, on the basis of a study (Ref 19). The heat treatment time was evaluated by hardness tests. After 9 h of heat treatment, the hardness values of the specimens

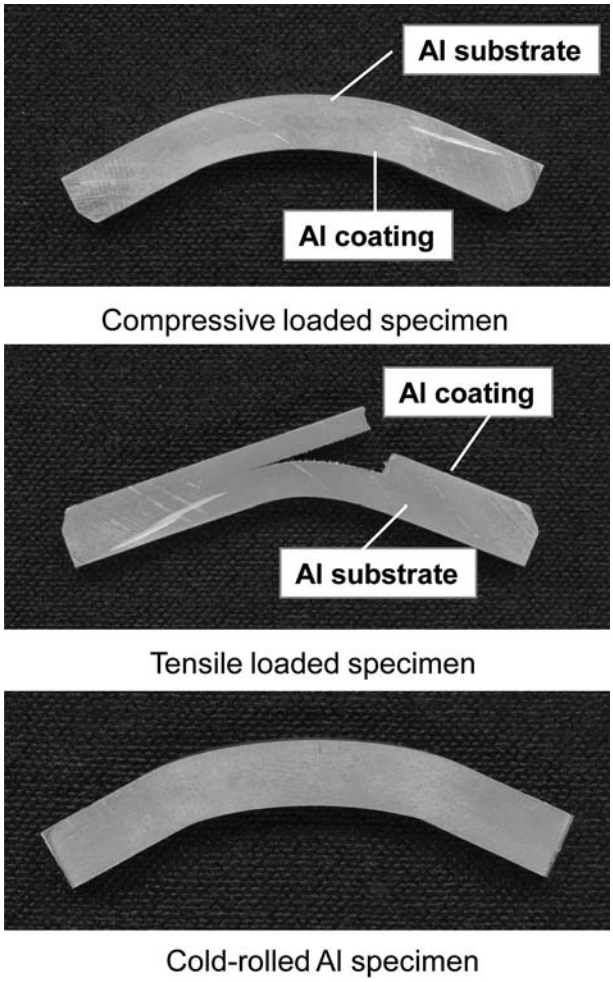

Fig. 11 Images of specimens after four-point bending tests

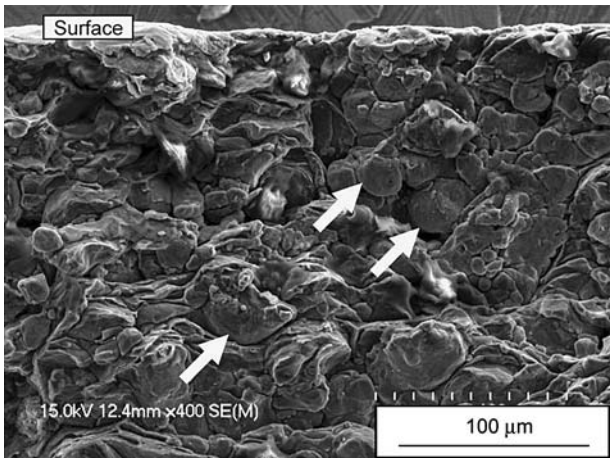

Fig. 12 Typical SEM image of fracture surface of tensile loaded specimen

became saturated. From this result, it was concluded that aluminum recrystallized after 9 h; therefore, the specimens were treated for 9 h.

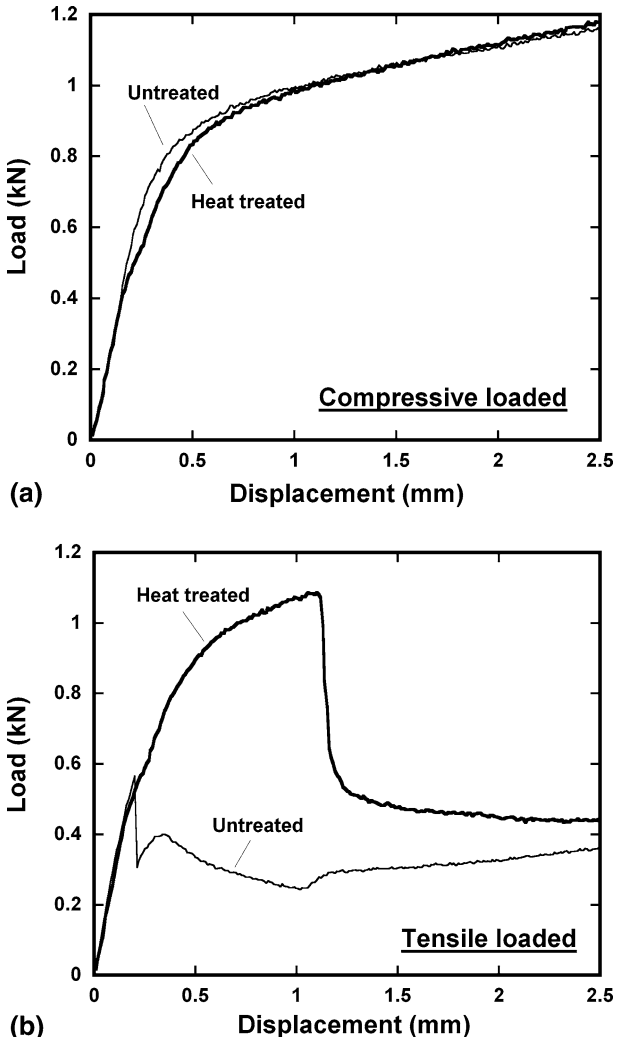

Fig. 13 Results of four-point bending tests of heat-treated specimens. (a) Compressive loaded and (b) Tensile loaded

The results of the four-point bending tests of the heat-treated (HT) specimens are shown in Fig. 13. In the case of compressive loading, the untreated specimens showed higher strength as compared to the HT specimens because of the decrease in the hardness value after heating. On the other hand, in the case of tensile loading, the HT specimens showed significantly higher strength and displacement as compared to the untreated specimens; the strength of the former is two times higher than that of the latter. Moreover, the displacement of the HT specimens is five times higher than the untreated specimens.

The typical SEM images of the fracture surfaces of the tensile loaded specimens after being subjected to the four-point bending tests are shown in Fig. 14. In the case of the untreated specimens, few particles remain on the fracture surface, leading to the unstable fractures. On the other hand, in the HT specimens, due to the formation of ductile fracture surfaces, their strength and displacement were improved dramatically.

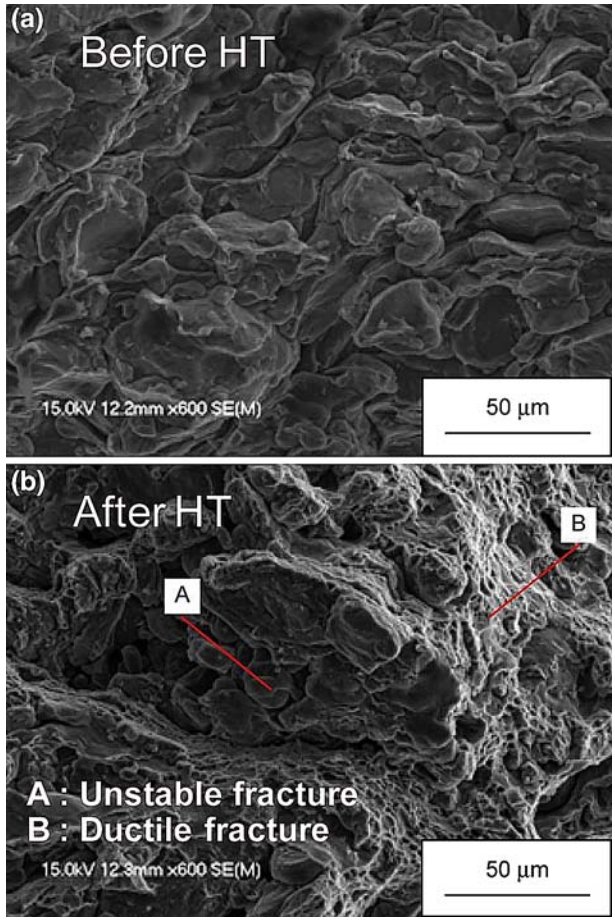

Fig. 14 Typical SEM images of fracture surface of heat-treated specimens after four-point bending tests

4. Conclusions

To evaluate the effects of surface conditions on aluminum deposition by the low-pressure cold-spray technique, the aluminum coatings on aluminum substrates have been characterized. The following main conclusions can be drawn:

1. In the case of low-pressure cold spraying, there is a time delay in particle deposition. This delay caused change in surface conditions, aiding particle deposition. During spraying, the substrate surface was exposed due to repeated impinging, resulting in the cleaning of the surface and formation of active newly formed surface.
2. The repeated impingements improve the deposition efficiency of particles. However, in the case of low-pressure cold spray, the deposition efficiency is very low, approximately 7%.
3. The repeated impingements enhance particle deposition. Hence, even though low-pressure cold spray exhibited low deposition efficiency, the velocity of particles deposited is lower than that in the case of

high-pressure cold spray. Further, the latter may not require repeated impingements because it has sufficient energy for formation of active newly formed surface due to the high-speed and high-pressure impingements. Accordingly, it is assumed that the difference in the critical velocities of the low- and high-pressure cold sprays is due to the difference in the mechanism of the active newly formed surface of the two techniques.

4. In the case of tensile loading, vertical cracks were formed in the aluminum coatings and the load value droped off sharply. However, the deposits have sufficient strength within the elastic region. Further, after heat treatment, the elongation of the specimens was improved.
5. Under compressive loading, the cold-sprayed specimens showed higher strength as compared to the cold-rolled aluminum specimen.
6. Under tensile loading, the heat-treated specimens showed significant improvement in strength and displacement. The strength of the HT specimens is two times higher than that of the untreated specimens. Moreover, the displacement of the former is five times longer than that of the latter.

Acknowledgments

This research was partially supported by the 21st COE Program ''The Exploration of the Frontiers of Mechanical Science Based on Nanotechnology,'' Tohoku University, by the Industrial Technology Research Grant Program, 2008, of the New Energy and Industrial Technology Development Organization (NEDO), Japan, and by Japan-France Integrated Action Program SAKURA.

References

1. A.P. Alkhimov, V.F. Kosarev, and A.N. Papyrin, A Method of Cold Gas-Dynamic Deposition, *Sov. Phys. Dokl.*, 1990, **35**, p 1047-1049
2. A.P. Alkimov, V.F. Kosarev, N.I. Nesterovich, and A.N.Papyrin, Method of Applying Coatings, Russian Patent No. 1618778, 8 Sept 1990
3. A.P. Alkhimov, A.N. Papyrin, V.F. Kosarev, N.I. Nesterovich, and M.M. Shushpanov, Gas-Dynamic Spray Method for Applying a Coating, U.S. Patent No. 5302414, 12 April 1994
4. A.P. Alkhimov, A.N. Papyrin, V.F. Kosarev, N.I. Nesterovich, and M.M. Shushpanov, Method and Device for Coating, European Patent No. 0484533 B1, 25 Jan 1995
5. A.P. Alkimov, A.N. Papyrin, V.F. Kosarev, N.I. Nesterovich, et al., Gas Dynamic Spraying Method for Applying a Coating, U.S. Patent No. 5302414, April 12, 1994, Re-examination Certificate, 25 Feb 1995
6. F. Leonardi, J.M. Ginder, and R.C. McCune, Method of Manufacturing Electromagnetic Devices Using Kinetic Spray, U.S. Patent No. 6592935, 15 July 2003
7. A.N. Papyrin, Cold Spray Technology, *Adv. Mater.*, 2001, **159**, p 49-51
8. W. Kroemmer, P. Heinrich, and P. Richter, Cold Spraying—Equipment and Application Trends, *Proceedings of the International Thermal Spray Conference 2003*, B.R. Marple and C. Moreau, Eds., May 5-8, 2003 (Orlando, FL), ASM International, 2003, p 97-102
9. R.E. Blose, T.J. Roemer, A.J. Mayer, D.E. Beatty, and A.N. Papyrin, Automated Cold Spray System: Description of Equipment and Performance Data, *Proceedings of the International Thermal Spray Conference 2003*, B.R. Marple and C. Moreau, Eds., May 5-8, 2003 (Orlando, FL), ASM International, 2003, p 103-111
10. J. Karthikeyan, and C.M. Kay, Cold Spray Technology: An Industrial Perspective, *Proceedings of the International Thermal Spray Conference 2003*, B.R. Marple and C. Moreau, Eds., May 5-8, 2003 (Orlando, FL), ASM International, 2003, p 117-121
11. H.Y. Lee, S.H. Jung, S.Y. Lee, Y.H. You, and K.H. Ko, Correlation Between Al_2O_3 Particles and Interface of Al–Al_2O_3 Coatings by Cold Spray, *Appl. Surf. Sci.*, 2005, **252**, p 1891-1898
12. H. Assadi, F. Gartner, T. Stoltenhoff, and H. Kreye, Bonding Mechanism in Cold Gas Spraying, *Acta Mater.*, 2003, **51**, p 4379-4394
13. T. Schmidt, F. Gartner, H. Assadi, and H. Kreye, Development of a Generalized Parameter Window for Cold Spray Deposition, *Acta Mater.*, 2006, **54**, p 729-742
14. A.N. Paryrin, S.V. Klinkov, and V.F. Kosarev, Modeling of Particle–Substrate Adhesive Interaction Under the Cold Spray Process, *Proceedings of the International Thermal Spray Conference 2003*, B.R. Marple and C. Moreau, Eds., May 5-8, 2003 (Orlando, FL), ASM International, 2003, p 27-35
15. R.C. Dykhuizen, M.F. Smith, D.L. Gilmore, R.A. Neiser, X. Jiang, and S. Sampath, Impact of High Velocity Cold Spray Particles, *J. Therm. Spray. Technol.*, 1999, **8**, p 559-564
16. J. Wu, H. Fang, S. Yoon, H.J. Kim, and C. Lee, The Rebound Phenomenon in Kinetic Spraying Deposition, *Scr. Mater.*, 2006, **54**, p 665-669
17. Y. Ichikawa, K. Ito, K. Ogawa, and T. Shoji, Deposition Mechanisms of Low Pressure Type Cold Sprayed Aluminum Coatings, *Surface Modification Technologies XXI*, 2007, p 497-506
18. K. Tanaka, M. Kumagai, and H. Yoshida, Dissimilar Joining of Aluminum Alloy and Steel Sheets by Friction Stir Spot Welding, *J. Jpn. Inst. Light Metals*, 2006, **56**, p 317-322 (in Japanese)
19. M. Tsuchida, H. Yoshida, and K. Hirano, Heat Treatment of Aluminum Alloys, *Sumitomo Metal Giho*, 1990, **31**, p 126-143 (in Japanese)